JOURNAL OF NANO- AND ELECTRONIC PHYSICS
Vol. 11 No 1, 01001(6pp) (2019)
ЖУРНАЛ НАНО- ТА ЕЛЕКТРОННОЇ ФІЗИКИ
Том 11 № 1, 01001(6cc) (2019)

Comparative *Ab initio* Calculations for ABO_3 Perovskite (001), (011) and (111) as well as $YAlO_3$ (001) Surfaces and *F* Centers

R.I. Eglitis*, A.I. Popov

Institute of Solid State Physics, University of Latvia, 8, Kengaraga Str., Riga LV1063, Latvia

(Received 22 November 2018; revised manuscript received 02 February 2019; published online 25 February 2019)

By means of the hybrid exchange-correlation functionals, we performed predictive *ab initio* calculations for industrially most important ABO_3 perovskites, like, $BaTiO_3$, $SrTiO_3$, $CaTiO_3$, $SrZrO_3$ and $PbZrO_3$ (001), (011) and (111) surfaces as well as bulk and (001) surface *F*-centers. From another side we performed comparative *ab initio* calculations for charged and polar $YAlO_3$ (001) surfaces. For $BaTiO_3$, CaTiO3, $SrZrO_3$ and $PbZrO_3$ perovskite neutral (001) surfaces, in most cases, all upper surface layer atoms relax inwards, whereas all second surface layer atoms relax upwards, and again, all third surface layer atoms relax inwards. The atom relaxation pattern for $YAlO_3$ polar and charged (001) surfaces is completely different from the ABO_3 perovskite neutral (001) surfaces. The ABO_3 perovskite (001) surface energies are practically equal for both AO and BO_2-terminations, and they are considerably smaller than (011) and especially (111) polar and charged surface energies. The atomic displacement magnitudes of nearest neighbor atoms around the (001) surface *F*-center in ABO_3 perovskites are considerably larger than the related displacement magnitudes of nearest neighbor atoms around the bulk *F*-center. In the ABO_3 perovskites the electron charge is considerably better localized inside the bulk *F*-center than in the (001) surface *F*-center, where the oxygen vacancy charge is more delocalized over the nearest neighbor atoms than in the bulk *F*-center case. The (001) surface *F*-center formation energy in the ABO_3 perovskites is smaller than the bulk *F*-center formation energy, which triggers the *F*-center segregation from the ABO_3 perovskite bulk towards its (001) surfaces. In most cases the (001) surface *F*-center induced defect level in the band gap of ABO_3 perovskites is located closer to the (001) surface conduction band bottom than the bulk *F*-center induced defect level to the bulk conduction band bottom.

Keywords: ABO_3 perovskites, $YAlO_3$, B3PW, F-center, (001) surfaces.

DOI: 10.21272/jnep.11(1).01001 PACS numbers: 68.35.Ct, 68.47.Gh

1. INTRODUCTION

Novel surface and interface phenomena, occurring in the ABO_3 perovskite and $YAlO_3$ (YAO) matrixes as well as their nanostructures, the complicated nature of their surface and interface states, the original mechanisms of electronic processes therein are the forefront topics in nowadays modern physics [1-8]. $PbTiO_3$ (PTO), $BaTiO_3$ (BTO), $CaTiO_3$ (CTO), $SrTiO_3$ (STO), $PbZrO_3$ (PZO), $BaZrO_3$ (BZO), $CaZrO_3$ (CZO) and $SrZrO_3$ (SZO) crystals belong to the so-called family of ABO_3 perovskites. ABO_3 perovskite surfaces are both of fundamental interest for classical basic research as well as they have a huge amount of technologically important applications, such as, for example, capacitors, actuators, charge storage devices, and many others [1-4], for which the quality of the surface and its structure are essential. From another side, the YAO has a high refractive index, mechanical resistance, optical transparency, chemical inertness and stability, which allows for YAO to be a prospective candidate for many optical applications [9-13].

Due to broad fundamental interest as well as extremely high technological importance during the last twenty years ABO_3 perovskite neutral (001) surfaces were worldwide intensively explored both experimentally and theoretically [14-16]. The technologically important YAO (001) surfaces are much more complicated than the neutral ABO_3 perovskite (001) surfaces, since they consist of alternating charged YO and AlO_2 layers. Of course, it is considerably more difficult to calculate, at the *ab initio* level, the ABO_3 perovskite very complex, polar and charged (011) [17-19] and (111) surfaces, than their neutral, and thereby rather simple, (001) surfaces [14-16].

It is worth to notice, that defects, for example, the oxygen vacancies, considerably affect all properties of the technologically important ABO_3 perovskite materials. In ABO_3 perovskites the single oxygen vacancy (V_0), or so-called neutral *F*-center, traps two electrons. Since the *F*-center is the best known classical point defect, which strongly affects all ABO_3 perovskite properties, their theoretical and experimental investigation is a very hot topic. Nevertheless, most of the experimental and theoretical studies in the ABO_3 perovskite materials are performed for the bulk *F*-center defects [20-29]. The BO_2 and especially AO-terminated ABO_3 perovskite (001) surface *F*-centers centers are considerably less studied both theoretically and experimentally.

The aim of work reported here was to create a unified theory, which describes systematic trends in ABO_3 perovskite and YAO (001), (011) and (111) surface as well as *F*-center in ABO_3 perovskite bulk and on its (001) surface calculations. Our calculation results were analyzed and systematic trends common for all ABO_3 perovskites as well as YAO were pointed out and systematized in a form easily accessible for a broad audience of readers.

2. COMPUTATIONAL METHOD

2.1 ABO_3 Perovskite and YAO Surface Calculations

We carried out our comprehensive *ab initio* calculations for ABO_3 perovskite and YAO surfaces using the

* rieglitis@gmail.com

hybrid exchange-correlation functionals B3PW or B3LYP as well as the world famous computer code CRYSTAL [30]. Important advantage of the CRYSTAL computer code is its ability to perform first principles calculations for isolated two-dimensional slabs perpendicular to the ABO_3 perovskite surface, without artificial periodicity in the z direction.

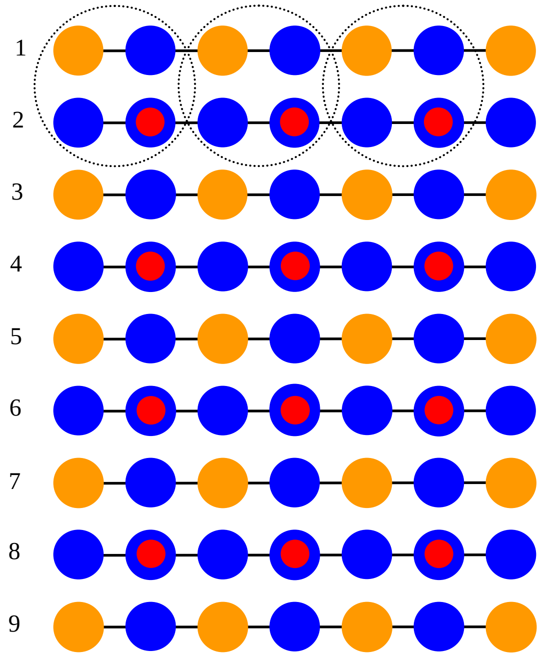

Fig. 1 – Side view of the PbO-terminated PTO (001) surface which contains 9 layers

We performed our calculations of ABO_3 perovskite and YAO (001) surfaces using symmetrical slabs consisting of nine alternating neutral AO and BO_2 (for ABO_3 perovskites), or charged YO and AlO_2 (in the case of YAO) layers. For ABO_3 perovskite case, our first slab was terminated by AO planes from both slab sides (Fig. 1) and consisted of 22 atoms containing supercell. Our second slab, in the case of ABO_3 perovskites, from both sides was terminated by BO2-planes and thereby consisted of 23 atoms containing supercell (Fig. 2). In our calculations, both AO and BO_2-terminated ABO_3 perovskite (001) slabs were non-stoichiometric, with their unit cell equations $A_5B_4O_{13}$ and $A_4B_5O_{14}$, respectively. In our ABO_3 perovskite (001) surface calculations, since they consist of neutral AO or BO_2-layers, we used standard basis sets for ions [30, 31]. In the case of YAO polar and charged (001) surface calculations, since they consist of charge layers (YO or AlO_2), assuming classical ionic charges ($+3e$) for Y and Al ions, and ($-2e$) for O ions, and taking into account that the supercell should be neutral in our calculations, we used basis sets for neutral Y, Al and O atoms [30, 31]. In order to characterize the ABO_3 perovskite and YAO chemical bonding and covalency effects, we used a classical Mulliken population analysis for the effective atomic charges Q and other local properties of the perovskite electronic structure. Additional calculation details for ABO_3 perovskite very complex, polar and charged (011) and (111) surfaces we described in references [17-19].

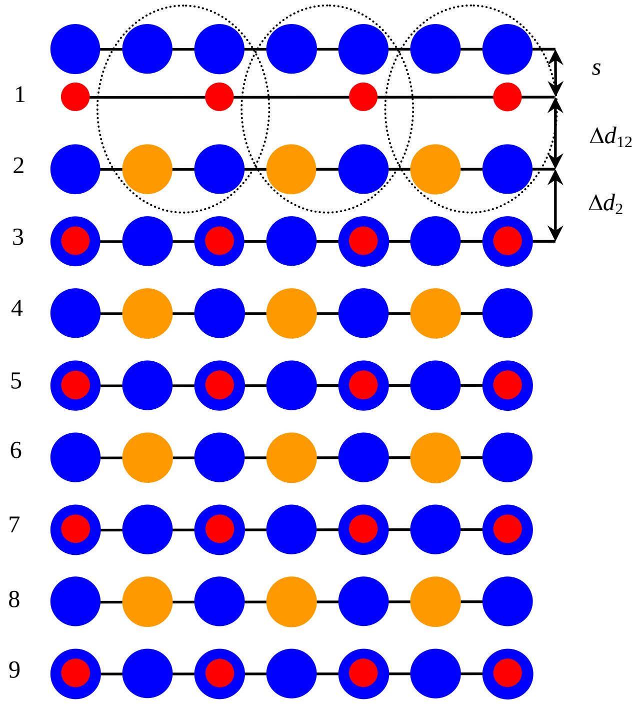

Fig. 2 – Side view of the TiO_2-terminated PTO (001) surface containing the definitions of the surface rumpling and the near-surface interplane distances

2.2 Surface Energy Calculations

With the aim to calculate the ABO_3 perovskite, for example, the PTO (001) surface energies, we started our calculations with the cleavage energy for unrelaxed PbO (Fig. 1) and TiO_2-terminated (001) surfaces (Fig. 2). It is worth to notice, that the ABO_3 perovskite surfaces with both terminations simultaneously arise under (001) cleavage of the crystal, and we adopt the convention that the cleavage energy is equally distributed between the created surfaces. In our calculations, the nine-layer PbO-terminated (001) slab with 22 atoms and the TiO_2-terminated slab with 23 atoms represent together nine bulk unit cells which together contain 45 atoms, so that

$$E_{surf}^{unr}(\mathrm{Y}) = ¼[E_{slab}^{unr}(\mathrm{PbO}) + E_{slab}^{unr}(\mathrm{TiO_2}) - 9E_{\mathrm{bulk}}], \quad (1)$$

where Y denotes PbO or TiO_2, $E_{slab}^{unr}(\mathrm{Y})$ are the unrelaxed energies of the PbO or TiO_2-terminated PTO (001) slabs, E_{bulk} is the energy per bulk unit cell, and the factor of ¼ comes from the fact that we create four surfaces upon the crystal cleavage event. Next, we can calculate the relaxation energies for each of PbO and TiO_2-terminations, when both sides of the slabs relax, according to the equation

$$E_{rel}(\mathrm{Y}) = ½[E_{slab}^{rel}(\mathrm{Y}) - E_{slab}^{unr}(\mathrm{Y})], \quad (2)$$

where $E_{slab}^{rel}(\mathrm{Y})$ is the slab energy after relaxation (and again Y = PbO or TiO_2). The surface energy consequently is defined as a sum of the cleavage and relaxation energies,

$$E_{surf}(\mathrm{Y}) = E_{surf}^{unr}(\mathrm{Y}) + E_{rel}(\mathrm{Y}) \quad (3)$$

In order to calculate the PTO (011) surface energies for the TiO and Pb-terminated (011) surfaces, we consider the cleavage of eight bulk unit cells (40 atoms) to result in the TiO and Pb-terminated slabs, containing 21 and 19 atoms. Also at this time we divide the cleavage energy equally between these two surfaces and obtain:

$$E_{surf}^{unr}(\mathrm{Y}) = ¼[E_{slab}^{unr}(\mathrm{Pb}) + E_{slab}^{unr}(\mathrm{TiO}) - 8E_{bulk}], \quad (4)$$

where Y means Pb or TiO, $E_{slab}^{unr}(\mathrm{Y})$ is the energy of the unrelaxed Pb or TiO-terminated (011) slab, and E_{bulk} is the $PbTiO_3$ energy per bulk unit cell.

Lastly, when we cleave the PTO crystal in another way, we obtain two identical O-terminated (011) surface slabs containing 20 atoms each. This allows us to simplify the calculations since the unit cell of the nine plane O-terminated (011) slab contains four bulk unit cells. Consequently, the surface energy is:

$$E_{surf}(\mathrm{O}) = ½[E_{slab}^{rel}(\mathrm{O}) - 4E_{bulk}], \quad (5)$$

where $E_{surf}(\mathrm{O})$ and $E_{slab}^{rel}(\mathrm{O})$ are the surface energy and the relaxed slab total energy for the O-terminated (011) surface.

3. CALCULATION RESULTS

3.1 *Ab initio* Calculations of ABO_3 and YAO Surfaces

As a starting point, we calculated the ABO_3 perovskite and YAO bulk lattice constants. Namely, using the B3PW hybrid exchange-correlation functional, we calculated the BTO and CTO bulk lattice constants (4.008 and 3.851Å, respectively). By means of the related B3LYP hybrid exchange-correlation functional we calculated the bulk lattice constants for the SZO (4.195Å), PZO (4.220Å) and YAO (3.712 Å). We used our theoretically calculated cubic bulk lattice constants in all our future ABO_3 perovskite and YAO numerical calculations.

As a next step, we performed hybrid exchange-correlation calculations for upper three layer atom relaxation for AO and BO_2-terminated neutral ABO_3 perovskite (001) surfaces as well as for very complex, charged and polar YO and AlO_2-terminated YAO (001) surfaces (Table 1). For the case of ABO_3 perovskites, according to our calculations, all upper layer atoms for both (001) terminations of all perovskites relax inwards in the direction towards the bulk. Just opposite, all ABO_3 perovskite second layer atoms relax outwards, with the single exception of second layer O atom for the SrO-terminated SZO (001) surface. All third layer atoms for both ABO_3 perovskite (001) terminations, again, relax inwards (Table 1).

The upper three layer atom relaxation pattern for charged and polar YO and AlO_2-terminated YAO (001) surfaces is quite different than for neutral ABO_3 perovskite (001) surfaces. The largest relaxation between all YAO and ABO_3 perovskite (001) surface atoms is our calculated inward displacement of the Y atom on the upper layer of the YO-terminated YAO (001) surface by 9.16 % of the YAO bulk lattice constant. The Y metal atom displacements on both YO and AlO_2-terminated YAO (001) surfaces always are larger than the related Al metal atom displacements.

Our calculated ABO_3 perovskite neutral (001) surface energies for both AO and BO_2-terminations are almost equal (Table 2). For example, for BTO and PZO perovskites, the AO-terminated (001) surface energies are slightly larger than the BO_2-terminated (001) surface energies by 0.12 and 0.07 eV, respectively. In the case of CTO and SZO perovskites, their BO_2-terminated (001) surface energies are slightly (by 0.19 and 0.11 eV, respectively) larger than their AO-terminated (001) surface energies. Our calculated complex charged and polar YAO (001) surface energies are considerably larger than all neutral ABO_3 (001) surface energies. It is worth to notice, that YAO polar and charge (001) surface energies are comparable with ABO_3 perovskite polar and charged (011) surface energies (Table 2). From Table 2 we can see that ABO_3 perovskite (011) and (111) surface energies are quite different for different (011) and (111) surface terminations. It is important to notice, that ABO_3 perovskite polar and charged (111) surface energies, independently of termination, are always considerably larger than the polar and charged (011) surface energies, but ABO_3 perovskite polar and charge (011) surface energies are always larger than their neutral (001) surface energies (Table 2).

3.2 *Ab initio* Calculations of *F*-centers in ABO_3 Matrix

From Table 3 we can see that two nearest to the *F*-center Ti atoms are repulsed from the oxygen vacancy in the $BaTiO_3$ matrix by 1.06 % of the BTO bulk lattice constant. The same relaxation pattern, according to the hybrid exchange-correlation functional calculations, is observed also in other ABO_3 perovskites, for example, $SrTiO_3$, $SrZrO_3$ and $PbZrO_3$, where the B atom is repulsed from the oxygen vacancy by 7.76, 3.68 and 0.48 % of the bulk lattice constant a_0. Just opposite, the second nearest neighbor O atoms in the ABO_3 perovskites are always attracted towards the *F*-center by 0.71, 7.79 and 2.63 % of a_0 in the BTO, STO and SZO matrixes.

Qualitatively the same relaxation pattern, but with considerably larger atomic displacements is observed also for the BO_2-terminated ABO_3 perovskite (001) surface *F*-centers. Namely, the B atoms are repulsed from the surface oxygen vacancies for the BO_2-terminated (001) surfaces of STO, SZO and PZO perovskites by 14, 9.17 and 8.46 % of the bulk lattice constant a_0. Again, the second nearest neighbor O atoms are attracted towards the surface oxygen vacancy on the BO_2-terminated STO and SZO (001) surfaces by slightly lager displacement magnitudes than in the bulk, namely, by 8 and 4.16 % of the lattice constant a_0. We performed also the first in the world hybrid exchange-correlation functional calculation for the *F*-center located on another, namely, BaO-terminated BTO (001) surface. Also in this case the nearest atom relaxation pattern around the surface *F*-center was qualitatively similar to the bulk and BO_2-terminated (001) surface *F*-center cases. Namely, the nearest to the BaO-terminated BTO (001) surface *F*-center Ti atoms are repulsed by 0.1 % of the a_0, whereas the second nearest oxygen atoms are attracted towards the surface *F*-center by 1.4 % of the a_0.

Inside the oxygen vacancy in the bulk of BTO, STO, SZO and PZO perovskites are concentrated – 1.103*e*, – 1.1*e*, – 1.25*e* and – 0.68*e* of additional charge. In the case of the ABO_3 perovskite (001) surface oxygen vacancy, electron charges are considerably more delocalized, than in the bulk *F*-center case. Namely, inside the oxygen vacancy on the BaO-terminated BTO (001) surface is located – 1.052*e*, which is less than in the BTO bulk oxygen vacancy – 1.103*e*. Also in the ZrO_2-terminated PZO (001) surface oxygen vacancy is located only – 0.3*e*, which is more than two times less than inside the PZO bulk oxygen vacancy – 0.68*e*.

In the ABO_3 perovskite bulk the *F*-center formation energy varies between 7 and 10 eV. For example, the ABO_3 perovskite bulk *F*-center formation energies for BTO, STO, SZO and PZO perovskites are equal to 10.3, 7.1, 7.55 and 7.25 eV. The *F*-center formation energy on the ABO_3 perovskite (001) surfaces is always smaller than in the bulk. Namely, the *F*-center formation energy on the BO_2-terminated STO, SZO and PZO (001) surfaces are equal to 6.22, 7.52 and 6.0 eV, respectively. According to our first in the world hybrid exchange-correlation calculation for the *F*-center formation energy on the BaO-terminated BTO (001), this formation energy is equal to 10.2 eV.

In the bulk of ABO_3 perovskites, the *F*-center defect induced levels in the band gap are located more close to the conduction band bottom, than to the valence band top. For example, in the BTO, STO, SZO and PZO perovskites, the *F*-center induced levels are located 0.23, 0.69, 1.12 and 1.72 eV below the conduction band bottom. In the case of (001) surface *F*-center induced defect levels for BTO, STO, SZO and PZO perovskites, they are located 0.07, 0.25, 0.93 and 2.58 eV below the conduction band bottom.

Table 1 – Our by means of B3PW or B3LYP hybrid exchange-correlation functionals calculated relaxation of (001) surface upper three layer atoms (in percent of bulk lattice constant) for BTO, CTO, SZO and PZO perovskites as well as YAO

Material		BTO	CTO	SZO	PZO	YAO
(001)-termination		BaO	CaO	SrO	PbO	YO
Layer	Ion	B3PW	B3PW	B3LYP	B3LYP	B3LYP
1	A	– 1.99	– 8.31	– 7.63	– 5.69	– 9.16
	O	– 0.63	– 0.42	– 0.86	– 2.37	1.89
2	B	1.74	1.12	0.86	0.57	– 0.32
	O	1.40	0.01	– 0.05	0.09	– 0.20
3	A	-	-	– 1.53	– 0.47	– 3.34
	O	-	-	– 0.45	– 0.47	– 0.03
(001)-termination		TiO_2	TiO_2	ZrO_2	ZrO_2	AlO_2
1	B	– 3.08	– 1.71	– 1.38	– 2.37	– 0.23
	O	– 0.35	– 0.10	– 2.10	– 1.99	– 0.55
2	A	2.51	2.75	2.81	4.36	0.48
	O	0.38	1.05	0.91	1.04	0.10
3	B	-	-	– 0.04	– 0.47	0.00
	O	-	-	– 0.05	– 0.28	– 0.01

Table 2 – Our by means of B3PW or B3LYP calculated BTO, CTO, SZO, PZO and YAO surface energies (in eV per surface cell)

Material	BTO	CTO	SZO	PZO	YAO
Termination	Surface energies for (001) surfaces				
AO	1.19	0.94	1.13	1.00	2.33
BO_2	1.07	1.13	1.24	0.93	3.31
	Surface energies for (011) surfaces				
BO	2.04	3.13	3.61	1.89	-
A	3.24	1.91	2.21	1.74	-
O	1.72	1.86	2.23	1.85	-
	Surface energies for (111) surfaces				
AO_3	8.40	5.86	9.45	8.21	-
B	7.28	4.18	7.98	6.93	-

Table 3 – B3PW calculated BTO, STO, SZO and PZO bulk and (001) surface *F*-center main characteristics

Bulk *F*-center main characteristics				
Material	BTO	STO	SZO	PZO
F-center charge inside vacancy (*e*)	– 1.103	– 1.1	– 1.25	– 0.68
F-center level under CB (eV)	0.23	0.69	1.12	1.72
F-center formation energy (eV)	10.3	7.1	7.55	7.25
B atom relaxation (% of a_0)	1.06	7.76	3.68	0.48
O atom relaxation (% of a_0)	– 0.71	– 7.79	– 2.63	-
A atom relaxation (% of a_0)	– 0.08	3.94	0.46	-5.99
BO_2-terminated (001) surface *F*-center main characteristics				
F-center charge inside vacancy (*e*)	-	-	– 1.10	– 0.3
F-center level under CB (eV)	-	0.25	0.93	2.58
F-center formation energy (eV)	-	6.22	7.52	6.0
B atom relaxation (% of a_0)	-	14	9.17	8.46
O atom relaxation (% of a_0)	-	– 8	– 4.16	-
A atom relaxation (% of a_0)	-	-	7.68	11.97
AO-terminated (001) surface *F*-center main characteristics				
F-center charge inside vacancy (*e*)	– 1.052	-	-	-
F-center level under CB (eV)	0.07	-	-	-
F-center formation energy (eV)	10.2	-	-	-
B atom relaxation (% of a_0)	0.1	-	-	-
O atom relaxation (% of a_0)	– 1.4	-	-	-
A atom relaxation (% of a_0)	1.0	-	-	-

4. CONCLUSIONS

With a few exceptions, the ABO_3 perovskite neutral (001) surface all upper layer atoms relax inwards, all second layer atoms relax upwards, and third layer atoms, again, relax inwards. The atom relaxation pattern for the YAO polar and charged (001) surfaces is quite different from the ABO_3 perovskite neutral (001) surfaces. The displacement magnitudes of all Y atoms on both the YO and AlO_2-terminated YAO (001) surfaces are always larger than the displacement magnitudes of all Al atoms on the both YAO (001) surfaces. The ABO_3 perovskite neutral (001) surface energies for both terminations AO and BO_2 are always almost equal. The ABO_3 perovskite polar and charged (111) surface energies are considerably larger than the polar and charge (011) surface energies. The neutral ABO_3 perovskite (001) surface energies are always smaller than the polar and charged (011) and especially (111) surface energies. The polar and charged YAO (001) surface energies are always considerably larger than the neutral ABO_3 perovskite (001) surface energies and they are comparable with the polar and charged ABO_3 perovskite (011) surface energies. The atomic displacements of the nearest neighbor atoms around the ABO_3 perovskite (001) surface *F*-center are considerably larger than the relevant nearest neighbor atomic displacements around the ABO_3 perovskite bulk *F*-center. As a rule, the ABO_3 perovskite (001) surface *F*-center electrons are considerably more delocalized, namely, less amount of electrons are trapped inside the ABO_3 perovskite (001) surface oxygen vacancy, than in the bulk *F*-center case in the ABO_3 perovskites. The energy difference between the BTO, STO, SZO and PZO typically smaller (001) surface *F*-center formation energies and larger bulk *F*-center formation energies in these materials triggers the *F*-center segregation from the ABO_3 perovskite bulk towards their (001) surfaces. In most cases (BTO, STO, SZO) the (001) surface *F*-center in ABO_3 perovskites induced defect level in the band gap is located more close to the conduction band bottom than for the bulk *F*-center case. The single exception is PZO, where the bulk *F*-center induced defect level is located closer to the conduction band bottom, than the (001) surface *F*-center induced defect level.

AKNOWLEDGEMENS

Authors R.I. Eglitis and A.I. Popov are grateful to the Joint Latvian-Ukrainian Research Project (the project No. LV-UA/2016/1) for financial support.

REFERENCES

1. Farokhipoor, B. Noheda, E. Snoeck, M. Hÿtch, *J. Phys. Cond. Matter.* **30**, 215701 (2018).
2. V.P. Savchyn, A.I. Popov, O.I. Aksimentyeva, H. Klym, Y.Y. Horbenko, V. Serga, A. Moskina, I. Karbovnyk, *Low Temp. Phys.* 42, 760 (2016).
3. S. Piskunov, R.I. Eglitis, *Solid State Ionics* **274**, 29 (2015).
4. A. Voloshynovskii, P. Savchyn, I. Karbovnyk, S. Myagkota, M. Cestelli Guidi, M. Piccinini, A.I. Popov, *Solid State Commun.* **149**, 593 (2009).
5. O.I. Aksimentyeva, V.P. Savchyn, V.P. Dyakonov, S. Piechota, Y.Y. Horbenko, I.Y. Opainych, P.Y. Demchenko, A. Popov, H. Szymczak, *Mol. Cryst. Liquid. Cryst.* **590**, 35 (2014).
6. A.S. Farlenkov, M.V. Ananyev, V.A. Eremin, N.M. Porotnikova, E.K. Kurumchin, B.T. Melekh, *Solid State Ionics* **290**, 108 (2016).
7. Y.G. Lyagaeva, D.A. Medvedev, A.K. Demin, T.V. Yaroslavtseva, S.V. Plaksin, N.M. Porotnikova, *Semicond.* **48**, 1353 (2014).
8. S. Piskunov, I. Isakoviča, A.I. Popov, *Opt. Mater.* **85**, 162 (2018).
9. S. Piskunov, I. Isakoviča, A.I. Popov, *Nucl. Instr. Meth. B* **434**, 6 (2018).
10. A.O. Matkovskii, D.I. Savytskii, D.Y. Sugak, I.M. Solskii, L.O. Vasylechko, Y.A. Zhydachevskii, M. Mond, K. Peterman, F. Wallrafen, *J. Cryst. Growth.* **241**, 455 (2002).
11. D. Sugak, A. Durygin, A. Matkovskii, A. Suchocki, I. Solskii, D. Savitskii, Y. Zhydachevskii, F. Wallrafen, K. Kopczynski, *Cryst. Res. Tech.* **36**, 1223 (2001).
12. Y. Zhydachevskyy, N. Martynyuk, A.I. Popov, D. Sugak, P. Bilski, S. Ubizskii, M. Berkowski, A. Suchocki, *J. Phys. Conf. Series* **987**, 012009 (2018).
13. E.A. Kotomin, R.I. Eglitis, J. Maier, E. Heifets, *Thin Solid Films* **400**, 76 (2001).
14. R.I. Eglitis, A.I. Popov, *J. Saudi. Chem. Soc.* **22**, 459 (2018).
15. M.G. Brik, C.G. Ma, V. Krasnenko, *Surf. Sci.* **608**, 146 (2013).
16. E. Heifets, J. Ho, B. Merinov, *Phys. Rev. B* **75**, 115431 (2007).
17. J. Wang, G. Tang, X.S. Wu, *Phys. Stat. Sol. B* **249**, 796 (2012).
18. J.A. Enterkin, A.K. Subramanian, B.C. Russell, M.R. Castell, K.R. Poeppelmeier, L.D. Marks, *Nature Mater.* **9**, 245 (2010).
19. E.A. Kotomin, V. Alexandrov, D. Gryaznov, R.A. Evarestov, J. Maier, *Phys. Chem. Chem. Phys.* **13**, 923 (2011).
20. W.J. Yin, S.H. Wei, M.M. Al-Jassim, Y. Yan, *Phys. Rev. B* **85**, 201201(R) (2012).
21. E.A. Kotomin, A.I. Popov, *Nucl. Instr. Meth. B* **141**, 1 (1998).
22. M. Sokolov, R.I. Eglitis, S. Piskunov, Y.F. Zhukovskii, *Int. J. Mod. Phys. B* **31**, 1750251 (2017).
23. J. Carrasco, F. Illas, N. Lopez, E.A. Kotomin, Y.F. Zhukovskii, R.A. Evarestov, Y.A. Mastrikov, S. Piskunov, J. Maier, *Phys. Rev. B* **73**, 064106 (2006).
24. A.I. Popov, E.A. Kotomin, J. Maier, *Nucl. Instr. Meth. Phys. Res. B* **268**, 3084 (2010).
25. E.A. Kotomin, R.I. Eglitis, A.I. Popov, *J. Phys. Condens. Matter.* **9**, L315 (1997).
26. P.W.M. Jacobs, E.A. Kotomin, R.I. Eglitis, *J. Phys. Condens. Matter.* **12**, 569 (2000).
27. R.I. Eglitis, S. Piskunov, *Comp. Cond. Matter.* **7**, 1 (2016).
28. S. Piskunov, A. Gopeyenko, E.A. Kotomin, Y.F. Zhukovskii, D.E. Ellis, *Comp. Mater. Sci.* **41**, 195 (2007).
29. E.A. Kotomin, S. Piskunov, Y.F. Zhukovskii, R.I. Eglitis, A. Gopeyenko, D.E. Ellis, *Phys. Chem. Chem. Phys.* **10**, 4258 (2008).
30. V.R. Saunders, R. Dovesi, C. Roetti, N. Causa, N.M. Harrison, R. Orlando, C.M. Zicovich-Wilson, *CRYSTAL-2009 User Manual* (University of Torino: Italy: 2009).
31. S. Piskunov, E. Heifets, R.I. Eglitis, G. Borstel, *Comp. Mater. Sci.* **29**, 165 (2004).

Порівняльні *Ab initio* розрахунки для перовскітів ABO_3 (001), (011) та (111), а також для $YAlO_3$ (001) поверхонь і *F* центрів

R.I. Eglitis, A.I. Popov

Institute of Solid State Physics, University of Latvia, 8, Kengaraga Str., Riga LV1063, Latvia

За допомогою гібридних обмінно-кореляційних функціоналів ми виконали прогнозні *ab initio* розрахунки для найбільш важливих у промисловому відношенні перовскітів ABO_3, таких як $BaTiO_3$, $SrTiO_3$, $CaTiO_3$, $SrZrO_3$ і $PbZrO_3$ (001), (011) та (111) поверхонь, а також і для об'ємних та (001) поверхневих *F*-центрів. З іншого боку проведено порівняння *ab initio* розрахунки для заряджених і полярних $YAlO_3$ (001) поверхонь. Для нейтральних (001) поверхонь перовскітів $BaTiO_3$, $CaTiO_3$, $SrZrO_3$ і $PbZrO_3$, у більшості випадків, усі атоми верхнього поверхневого шару релаксують всередину, тоді як усі атоми другого поверхневого шару релаксують угору, і, знов, усі атоми третього поверхневого шару релаксують всередину. Картина релаксації атомів для полярної і зарядженої $YAlO_3$ (001) поверхонь повністю відрізняється від картини для нейтральних (001) поверхонь перовскітів ABO_3. Поверхневі енергії перовскітів ABO_3 (001) практично однакові як для AO, так і для BO_2 граничних поверхонь, і вони значно менші поверхневих енергій полярних і заряджених (011) та, особливо, (111) поверхонь. Величини атомних зміщень найближчих сусідніх атомів навколо (001) поверхневого *F*-центру в перовскітах ABO_3 суттєво перевищують відповідні величини зміщень найближчих сусідніх атомів навколо об'ємного *F*-центру. Для перовскітів ABO_3, заряд електронів значно краще локалізований всередині об'ємного *F*-центру, ніж у (001) поверхневому *F*-центрі, де вакансії кисню більш делокалізовані між найближчими сусідніми атомами. Енергія формування (001) поверхневого *F*-центру в перовскітах ABO_3 менша за енергію формування об'ємного *F*-центру, яка ініціює сегрегацію *F*-центрів з об'єму перовскіту ABO_3 до його (001) поверхні. У більшості випадків, енергетичний рівень дефектів, який зумовлений (001) поверхневим *F*-центром, в забороненій зоні перовскитів ABO_3 розташований ближче до дна зони провідності поверхні (001), у той час як рівень, який зумовлений об'ємними *F*-центрами, розташований ближче до дна об'ємної зони провідності.

Ключові слова: Перовскіти ABO_3, $YAlO_3$, B3PW, *F*-центр, (001) поверхні.